

# Parallel syndrome extraction with shared flag qubits for Calderbank-Shor-Steane codes of distance three

Pei-Hao Liou<sup>1,\*</sup> and Ching-Yi Lai<sup>1,2,†</sup>

<sup>1</sup>*Institute of Communications Engineering, National Yang Ming Chiao Tung University, Hsinchu 30010, Taiwan*

<sup>2</sup>*Physics Division, National Center for Theoretical Sciences, Taipei 10617, Taiwan*

(Dated: February 20, 2023)

To perform achieve fault-tolerant quantum computation, one can use flagged syndrome extraction with fewer ancilla qubits. However, it suffers from long circuit depth if one stabilizer is measured at a time. Previously, Reichardt showed that it is possible to measure multiple stabilizers with at most one shared flag qubit for certain small quantum codes. In this paper, we propose a procedure for general Calderbank-Shor-Steane codes of distance three so that multiple  $Z$ -stabilizers ( $X$ -stabilizers) can be fault-tolerantly measured in parallel with one shared flag qubit. We simulate the memory and computation pseudo-thresholds for various code schemes. In particular, our parallel scheme based on Shor's nine-qubit code performs better than known seven- and nine-qubit schemes in the literature.

## I. INTRODUCTION

Physical platforms for quantum computing usually have finite qubit coherent time and high gate error rates [1–4]. To have reliable quantum computers, it is necessary to realize fault-tolerant quantum computation (FTQC) [5–12]. The central idea of FTQC is to compute directly on quantum states encoded in a quantum error-correcting code. Encoded logical operations are implemented and quantum error corrections are constantly applied, so that an arbitrarily accurate quantum computation is possible when the error rates of physical gates are below a certain threshold [5].

To perform a fault-tolerant syndrome extraction for error correction, one may use one of the Shor, Steane, and Knill syndrome extraction procedures [6, 11, 13]. Usually repeated syndrome measurements are performed with the Shor syndrome extraction [6] to obtain a reliable error syndrome. One may also design quantum data-syndrome codes to handle syndrome measurement errors [14, 15]. If the Steane or Knill syndrome extraction is used, no repeated measurements are required since one has to handle only an effective error and a residual error will be treated in the next error correction cycle [16]. However, large ancilla blocks are required for the Steane or Knill syndrome extraction. Huang and Brown recently proposed another syndrome extraction method, which is a compromise of both the Shor and the Steane extractions [17].

It is also possible to perform error correction for certain quantum codes with direct syndrome extractions [18, 19] but usually a decoding strategy is required, such as repeated syndrome measurements followed by a perfect matching.

In [20], Yoder and Kim showed that fewer ancilla qubits are required for FTQC based on certain quantum

codes. Following that, Chao and Reichardt introduced the idea of flag qubits for syndrome extraction so that fewer ancilla qubits are required for a syndrome extraction procedure to be fault-tolerant [21, 22]. They also showed that multiple stabilizers can be measured with one shared flag qubit for certain small codes. The central idea is to enlarge the space of syndrome bits by introducing additional flag qubits and controlled-Not (CNOT) gates such that any single location failure will have a unique error syndrome and thus can be corrected. Since a flag FTQC scheme requires fewer qubits, it is suitable for near-term quantum devices. More general flag schemes have been studied for FTQC based on stabilizer codes and magic state distillation [23–26].

A standard flagged syndrome extraction circuit measures a single stabilizer generator at a time. If a complete syndrome extraction circuit is composed of several flagged syndrome extraction circuits in a cascade form, most qubits are idle most of the time. When the error rate for idling is high, the benefit of using fewer ancilla qubits with the flagged syndrome extraction may be compensated. To handle this problem of long circuit depth, Reichardt proposed the idea of flagged syndrome extraction for multiple stabilizers with shared flag qubits for certain small codes of distance three [27]. Moreover, he showed that two or three stabilizer of the  $[[7,1,3]]$  code [28] can be fault-tolerant measured in parallel without additional flag qubits. (Reichardt's protocol is reviewed in Appendix A.)

In this paper, we propose a procedure (Algorithm 2) for parallel syndrome extraction with shared flag qubits for a general Calderbank-Shor-Steane (CSS) code of distance three. We show that multiple  $Z$ -stabilizers can be measured with one shared flag qubit and similarly for multiple  $X$ -stabilizers. In this way, the circuit depth can be greatly reduced compared to the standard flagged syndrome extraction. In particular, we show that all the  $Z$ -stabilizers ( $X$ -stabilizers) can be measured in parallel with one flag qubit in the scenario of fault-tolerant error detection.

In addition, we show that for flagged syndrome ex-

\* phliou.ee08@nycu.edu.tw

† cylai@nycu.edu.tw

traction of a CSS code, a complete unflagged syndrome extraction is not necessary when a flag rises. More precisely, we observe that in a parallel syndrome extraction of multiple  $Z$ -stabilizers, the residual errors when a flag rises will have at most a weight-one Pauli  $X$  error, which can be corrected in the next error correction cycle, so only  $X$ -stabilizers need to be measured to catch high-weight  $Z$  errors. In this way, the circuit depth can be further reduced. Accordingly, we propose Algorithm 3 that decodes flagged scheme of CSS codes in an adaptive way.

We remark that one  $X$ -stabilizer and one  $Z$ -stabilizer (two dual operators) can be measured in parallel with a shared flag qubit using Reichardt's method for the  $[[15,7,3]]$  code. On the contrary, our procedure applies to only stabilizers of the same type. Thus our procedure applies to asymmetric CSS codes with unequal numbers of  $X$ - and  $Z$ -stabilizers, such as the  $[[15,1,3]]$  Reed-Muller code.

Finally, we simulate and compare several flag and parallel schemes based on the  $[[4,2,2]]$ ,  $[[7,1,3]]$ , and Shor's  $[[9,1,3]]$  [29] codes for error detection and error correction, respectively. Both the memory and computation pseudo-thresholds are simulated for each scheme. Note that we do not assume a two-dimensional layout for a FTQC scheme with physical restrictions [30–32] and non-local CNOTs are allowed.

We observe that a parallel scheme will perform better than its nonparallel counterpart. In particular, our  $[[9,1,3]]$  parallel scheme has the memory pseudo-thresholds of  $9.82 \times 10^{-3}$  when the memory is error-free and  $8.84 \times 10^{-4}$  when all the gate and memory error rates are the same. These numbers are better than those obtained by Reichardt's  $[[7,1,3]]$  parallel scheme (see Table IV).

We also compare our  $[[9,1,3]]$  parallel scheme with known nine-qubit code schemes in the literature. In [19], Li et al. proposed a fault-tolerant quantum memory scheme for the  $[[9,1,3]]$  Bacon-Shor code using only four ancilla qubits, called *Bacon-Shor-13* and they showed this scheme outperforms a scheme based on the  $[[9,1,3]]$  surface codes using eight ancilla qubits. From the circuit design, one can observe that Bacon-Shor-13 performs better when the memory rate is low since it has fewer qubits involved (a total of 13 qubits).

As can be seen in Table IV, our  $[[9,1,3]]$  parallel scheme outperforms Bacon-Shor-13 in both the memory and the computation pseudo-thresholds.

This paper is organized as follows. In Section II, we briefly introduce the basics of stabilizer codes, FTQC, and flagged syndrome extraction. In Section III, we show how to perform parallel syndrome extraction for multiple stabilizers of a CSS code with one shared flag qubit. Simulations our parallel schemes are provided and compared in Section IV. Then we conclude in Section V.

## II. PRELIMINARIES

### A. Stabilizer Codes

We consider quantum errors that are tensor product of Pauli matrices  $I = \begin{pmatrix} 1 & 0 \\ 0 & 1 \end{pmatrix}$ ,  $X = \begin{pmatrix} 0 & 1 \\ 1 & 0 \end{pmatrix}$ ,  $Y = \begin{pmatrix} 0 & -i \\ i & 0 \end{pmatrix}$ , and  $Z = \begin{pmatrix} 1 & 0 \\ 0 & -1 \end{pmatrix}$  in the computational basis  $\{|0\rangle, |1\rangle\}$ . For convenience, we omit the symbol of tensor product for  $n$ -fold Pauli operators. In addition, we may sometimes omit the identity  $I$  and use an index to indicate which qubit a Pauli matrix operates on. For example,  $X \otimes Y \otimes Z \otimes I \otimes I$  will be denoted as  $X_1 Y_2 Z_3$ . An  $X$ - or  $Z$ -type Pauli operator has nonidentity components that are all  $X$  or all  $Z$  matrices. For an  $X$ - or  $Z$ -type Pauli operator, the redundant  $X$ s or  $Z$ s will be suppressed. For example,  $X_1 X_2 X_3$  may also be denoted as  $X_{1,2,3}$ . The *weight* of an  $n$ -fold Pauli operator is the number of its nonidentity elements. Usually a high-weight error is less likely than a low-weight error in an error model. Consequently, we would like to handle the more-likely events in error correction.

An  $[[n, k, d]]$  stabilizer code  $C(\mathcal{S})$  is defined as the joint  $+1$  eigenspace of an Abelian subgroup  $\mathcal{S}$  of the  $n$ -fold Pauli operators with  $n - k$  independent generators  $g_1, \dots, g_{n-k}$  and the operators in  $\mathcal{S}$  are called *stabilizers*. It encodes  $k$  logical qubits into  $n$  physical qubits and can detect errors up to weight  $d - 1$  or correct errors up to weight  $\lfloor \frac{d-1}{2} \rfloor$  [9].

**Definition 1** The *error syndrome* of a Pauli error  $E$  with respect to the  $n - k$  stabilizer generators  $g_i \in \mathcal{S}$  is a binary string of length  $n - k$ , whose  $i$ -th bit is 0 if  $E$  commutes with  $g_i$ , and 1, otherwise.

If an error has a nonzero error syndrome, it can be detected and possibly corrected.

**Proposition 2** If each operator of a set of Pauli errors has a unique error syndrome with respect to a stabilizer group, then this set of Pauli errors is correctable.

Clearly one can build a *lookup table* that consists of each error operator and its error syndrome for error correction [33].

A CSS code is a stabilizer code defined by  $X$ -type or  $Z$ -type stabilizer generators [34, 35].  $X$  and  $Z$  errors can be separately treated in a CSS code. A CSS code of distance three can correct a single  $X$  error and a single  $Z$  error, simultaneously.

### B. Fault-tolerant quantum computation

In a quantum circuit, quantum errors occur due to imperfect quantum gates or memory and they may propagate through multiple-qubit gates.

**Definition 3** A *location failure* is referred to as an event that a Pauli error occurs after a perfect single-qubit gate, two-qubit gate, ancilla preparation, qubit measurement, or an idle qubit in a circuit.

To perform quantum computation with imperfect gates and memory, quantum information has to be encoded in a quantum stabilizer code, and encoded quantum operations are performed so that quantum error correction is constantly performed.

**Definition 4** A location in a procedure is called a *bad location* if one of its location failures may evolve into an uncorrectable (respectively, undetectable) error for a code of distance three (respectively, two). Such location failures are called *bad location failures*.

**Definition 5** A procedure is called *fault-tolerant* if there are no bad locations in the procedure.

For example, a fault-tolerant circuit of a CNOT gate on two qubits is encoded to the circuit in Fig. 1 where each qubit is encoded into a CSS codeword and bitwise CNOT gates are applied. Note that an error detection (ED) or error correction block is performed to each codeword prior to and subsequent to the bitwise CNOT gates. Such implementation of a logical CNOT gate is called an *extended rectangle (ex-Rec)* of the CNOT gate [36].

**Definition 6** The *error threshold* for a procedure is the (physical) error rate below which the logical error rate of the procedure would be lower than the error rate.

We consider two types of thresholds: *memory threshold* and *computation threshold*. The memory threshold is the error threshold for error correction or detection on a quantum codeword. The computation threshold is the error threshold for an ex-Rec CNOT gate since the ex-Rec CNOT is usually the most complicated procedure in a universal set of gates.

Simulations in this paper assume the following error model. We add independent depolarizing errors with rate  $p$  as quantum operations after gates or before measurements in the circuit. Assume that each gate takes the same unit of time. Each single-qubit location undergoes  $X$ ,  $Y$ , or  $Z$  with probability  $p/3$  and each qubit-measurement is corrupted with probability  $2p/3$ . Each CNOT gate is followed by one of the 15 non-identity two-qubit Pauli operators with probability  $p/15$ . An idle qubit suffers depolarizing errors with rate  $\gamma p$  for  $0 \leq \gamma \leq 1$ .

### C. Fault-tolerant syndrome extraction with flag qubits

In general a syndrome extraction circuit has many bad locations. By introducing additional ancillary qubits, called *flag qubits*, one can carefully place controlled-NOT

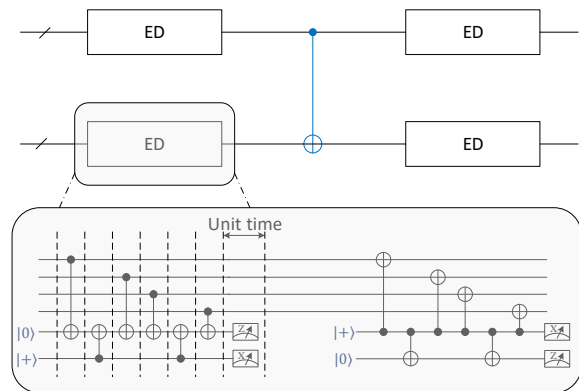


FIG. 1. The ex-Rec CNOT for the  $[[4,2,2]]$  code with flagged syndrome extraction. Two quantum codewords encoded by the  $[[4,2,2]]$  code are first processed by two error detection (ED) blocks. Then bitwise CNOT gates (colored in blue) are applied, followed by another two ED blocks. A fault-tolerant ED block circuit measures the two stabilizers  $ZZZZ$  and  $XXXX$  for the  $[[4,2,2]]$  code. In this example, flagged syndrome extraction is used, which is explained in Fig. 2.

(CNOT) gates so that bad location failures will trigger these flag qubits, and thus, be detected [21, 22].

Figure 2 (a) illustrates how a weight-4 stabilizer  $Z_1Z_2Z_3Z_4$  is measured. Four CNOT gates are used to check the parity of four data qubits and the result is left in the first ancilla qubit (marked in red), which is initialized in  $|0\rangle$ . Observe that location  $a$  in Fig. 2 (a) is a bad location since a  $Z$  error here will induce a weight-2  $Z$  error on the data qubits. This event cannot be detected by the stabilizer measurements but it will be detected using a flag qubit with elegantly positioned CNOT gates (marked in blue) as shown in Fig. 2 (a). We say that this failure triggers the flag qubit and the flag rises. This method is called *flagged syndrome extraction* [21, 22]. The syndrome extraction circuit without the flag qubit and the two CNOT gates will be called an *unflagged syndrome extraction circuit*.

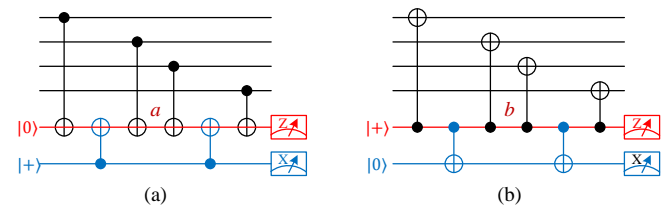


FIG. 2. (a) Flagged fault-tolerant syndrome extraction for  $Z_1Z_2Z_3Z_4$ . The ancilla qubit initialized in  $|+\rangle$  is a flag qubit, which is coupled to the raw syndrome measurement circuit via two additional CNOTs. (b) Flagged fault-tolerant syndrome extraction for  $X_1X_2X_3X_4$ .

The measurement of a weight-4 stabilizer  $X_1X_2X_3X_4$  is similarly implemented in Fig. 2 (b). These circuits can be directly generalized for measuring  $Z$ - or  $X$ -stabilizers of higher weight as shown in Fig. 3. This is called a

*standard flagged syndrome extraction circuit.* A circuit for measuring the error syndrome with respect to a set of stabilizer generators will be called a *complete syndrome extraction circuit*.

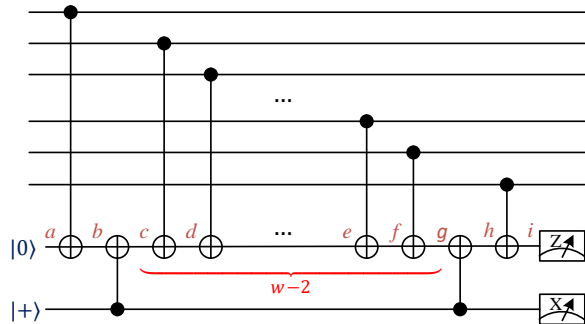


FIG. 3. Standard flagged syndrome extraction for a  $Z$ -type stabilizer of weight  $w$ .

In the following, we discuss how flagged syndrome extraction is used in fault-tolerant quantum error detection and correction.

### 1. Quantum error detection with flag qubits

A fault-tolerant error-detection scheme has to be designed such that a detectable error will not evolve into an undetectable error. A flagged syndrome extraction circuit ensures that any bad location failure will trigger a flag qubit and be detected. Therefore, one learns that some error occurs if any one of the measurement outcomes in the flagged syndrome extraction circuits is  $-1$ , and the codeword has to be discarded.

Consider the  $[[4, 2, 2]]$  error-detecting code [9], which is defined by two stabilizer generators  $X_1X_2X_3X_4$  and  $Z_1Z_2Z_3Z_4$ . Its complete syndrome extraction consists a sequential implementation of Figs. 2 (a) and 2 (b) as shown in Fig. 1. This procedure is fault-tolerant.

### 2. Quantum error correction with flag qubits

In a fault-tolerant error correction scheme with flagged syndrome extraction, error recovery is adaptively performed according to the measured error syndrome and flag qubits. The basic error correction rules for distance-three quantum codes are as follows.

A complete flagged syndrome extraction circuit is first implemented.

If no flag qubits rise, it is most likely that no bad location failure occurs, and a usual syndrome decoding is performed according to the measured error syndrome. If one flag qubit rises during the complete syndrome extraction, a round of complete unflagged syndrome extractions will be performed right away, and error recovery is per-

formed according to the flag qubit as well as its measured error syndrome.

When a flag qubit rises, we know that there is some high-weight error in the codeword. In this case, the conventional minimum-weight decoding rule does not work, and we are not aware of any general decoding algorithm. We have to choose the most likely error according to the flag qubits and the error syndrome from a complete unflagged syndrome extraction.

Let  $f \in \{0, 1\}^r$  be the measurement outcomes on the flag qubits in a complete flagged syndrome extraction circuit with  $r$  flag qubits. We denote  $\text{LOOKUP}(f)$  as the syndrome look-up table according to the flag outcomes  $f$ . Note that  $\text{LOOKUP}(0)$  is the original syndrome table.

The standard decoding procedure for flagged syndrome extraction in Ref. [21] is summarized in Algorithm 1.

---

#### Algorithm 1: Standard decoding procedure for flagged syndrome extraction.

---

- 1 Suppose that there are  $r$  stabilizer generators  $g_1, g_2, \dots, g_r$  and  $f$  is initialized to  $0^r$ ;
  - 2 **for**  $i = 1, 2, \dots, r$  **do**
  - 3     Apply  $C(g_i)$  and get syndrome bit  $m_i$ ;
  - 4     Update  $f_i$  according to the measurement outcome on the flag qubit in  $C(g_i)$ ;
  - 5     **if**  $f_i = 1$  **then**
  - 6         Apply a complete unflagged syndrome extraction circuit to get syndrome bits  $m' \in \{0, 1\}^r$ ;
  - 7         Perform error correction according to  $\text{LOOKUP}(f)$  and  $m'$ ;
  - 8         **break**;
  - 9     **else if**  $m_i = 1$  **then**
  - 10         Apply a complete unflagged syndrome extraction circuit to get syndrome bits  $m' \in \{0, 1\}^r$ ;
  - 11         Perform error correction according to  $\text{LOOKUP}(0)$  and  $m'$ ;
  - 12         **break**;
  - 13     **end**
  - 14 **end**
- 

### III. FLAG-SHARED SYNDROME EXTRACTION FOR CODES OF DISTANCE TWO OR THREE

In this section, we propose a procedure for parallel syndrome extraction with shared flag qubits for a general CSS code of distance three. We begin with the notation.

#### A. Parallel flagged syndrome extraction with one shared flag qubit

Suppose that there are  $r$  stabilizer generators  $g_1, \dots, g_r$  to be measured for an  $[[n, k, 3]]$  CSS code. Let  $C(g_i)$  be a (standard) flagged syndrome extraction circuit for  $g_i$  as

shown in Fig. 3 for a  $Z$ -stabilizer. The flagged syndrome extraction circuit is designed so that each bad location failure will trigger the flag qubit. Let  $B(C(g_i))$  denote the number of location failures in  $C(g_i)$  that will trigger the flag qubit.

An observation is that  $B(C(g_i))$  depends on the weight of the stabilizer  $g_i$ .

**Proposition 7** Suppose that  $g_i$  is an  $X$ - or  $Z$ -stabilizer of weight  $w$ . Then  $B(C(g_i)) \leq w - 1$ .

**Proof.** Consider a  $Z$ -stabilizer  $g_i$  of weight  $w$  with a standard flagged syndrome extraction circuit  $C(g_i)$  as shown in Fig. 3. There are two CNOTs connecting the flag and the ancillary qubits. Other  $w - 2$  CNOTs are placed in sequence between these two CNOT gates. All the location failures at  $a, b, h$ , and  $i$  will not trigger the flag qubit, whereas a Pauli  $Z$  (or  $Y$ ) at the other  $w - 1$  locations  $c, d$ , up to  $g$  will.

Note that a  $Z$  error at  $g$  is not a bad failure since it remains to be a weight-one error at the end of the circuit. The other  $w - 2$  location failures may evolve to high-weight  $Z$  errors, which are potential bad failures.

Another observation is that flagged syndrome extraction circuits for stabilizers of the same type may be joined together and a shared flag qubit may be sufficient for fault-tolerant syndrome extraction. For example, Fig. 4 part (B) shows the joint flagged syndrome extraction circuit with one shared flag qubit for two stabilizers.

Moreover, we find that no additional bad location failures are introduced in this joint circuit. Consider the two CNOTs connecting an ancilla qubit and the flag qubit. A  $Z$  error on the flag qubit prior to the first CNOT will be absorbed to the flag qubit, An  $X$  error on the flag qubit will not propagate to any other ancillas, and it triggers the flag qubit. A  $Z$  error on the flag qubit following the second CNOT has no effect on the flag qubit. An  $X$  error on the flag qubit will not propagate to any other ancillas, and it triggers the flag qubit. No errors on one ancilla could propagate through the flag qubit to another ancilla because of the directions of CNOTs. Hence, we have the following proposition.

**Proposition 8** Suppose that  $g_{j_1}, \dots, g_{j_s}$  are stabilizers of the same type ( $X$  or  $Z$ ). Suppose that a flag qubit is shared by  $C(g_{j_1}), \dots, C(g_{j_s})$  and the CNOTs connecting the ancillas and the flag qubit are placed in sequence. Then a bad location failure in this joint circuit must have appeared in one of the  $C(g_{j_i})$ s; no additional bad location failure is introduced in the joint circuit.

The next question is: how many stabilizer generators can be fault-tolerantly measured in parallel with only one shared flag qubit? Suppose that there are  $x$   $X$ -type stabilizers and  $z$   $Z$ -type stabilizers. If  $g_i$  is a  $Z$ -stabilizer, we observe that in  $C(g_i)$ , a bad location failure always evolves to a high-weight  $Z$  error. For example, in Fig. 2 (a) a  $Z$  error at location  $a$  evolves to  $Z_3Z_4$  at the end of the circuit. When a flag rises, this high-weight  $Z$

error will be identified by measuring the  $X$ -stabilizers in an unflagged syndrome extraction circuit. Consequently, we must have  $B(C(g_i)) \leq 2^x$  so that all the location failures that trigger the flag qubit can be identified using an unflagged syndrome extraction. Similar for the flagged syndrome extraction of an  $X$ -stabilizer.

Consequently, we must have the following proposition for a flag-shared syndrome extraction scheme of multiple stabilizers of the same type, following Proposition 8.

**Proposition 9** Suppose that  $g_{j_1}, g_{j_2}, \dots, g_{j_s}$  are stabilizers of the same type and  $C(g_{j_1}), C(g_{j_2}), \dots, C(g_{j_s})$  can be performed in parallel using a shared flag qubit. Then the following conditions hold.

1. Each distinct bad location failure has a unique error syndrome when a flag rises.
2. 
$$\begin{cases} \sum_{i=1}^s B(C(g_{j_i})) \leq 2^z, & \text{if } g_{j_1}, \dots, g_{j_s} \text{ are } X\text{-type;} \\ \sum_{i=1}^s B(C(g_{j_i})) \leq 2^x, & \text{if } g_{j_1}, \dots, g_{j_s} \text{ are } Z\text{-type,} \end{cases}$$
 assuming that there are  $x$   $X$ -type stabilizers and  $z$   $Z$ -type stabilizers.

According to Propositions 7, 8, and 9, we have a procedure (Algorithm 2) for finding a parallel flagged syndrome extraction circuit for a set of stabilizers with a shared flag qubit.

---

**Algorithm 2:** Finding a parallel flagged syndrome extraction circuit with one shared flag qubit.

---

- 1 Choose stabilizers  $g_{j_1}, g_{j_2}, \dots, g_{j_s}$  of  $Z$  ( $X$ ) type such that  $\sum_{i=1}^s B(C(g_{j_i})) \leq 2^x$  ( $2^z$ ), where  $x$  ( $z$ ) is the number of independent  $X$  ( $Z$ ) stabilizer generators;
  - 2 Let  $C(g_{j_1}), C(g_{j_2}), \dots, C(g_{j_s})$  share one flag qubit;
  - 3 Let *unique* = *false*;
  - 4 **while** *unique* **do**
  - 5     randomly adjust the orders of a subset of CNOTs in  $C(g_{j_1}), C(g_{j_2}), \dots, C(g_{j_s})$ ;
  - 6     **if** *each of the locations that trigger the flag qubit has a unique error syndrome from an unflagged syndrome extraction*;
  - 7     **then**
  - 8         let *unique* = *true*;
  - 9     **end**
  - 10 **end**
- 

We remark that the number of possible error syndromes is exponential in the number of stabilizer generators, whereas the number of locations that trigger the flag qubit is linear in the number of stabilizer generators in parallel. As a consequence, this randomized algorithm is good enough when  $x$  or  $z$  is sufficiently large. We provide examples of Shor's  $[[9,1,3]]$  code and the  $[[15,1,3]]$  (punctured) Reed-Muller code in the following subsections.

We can extend the above idea for error detection. Note that the conditions for error detection is that any bad

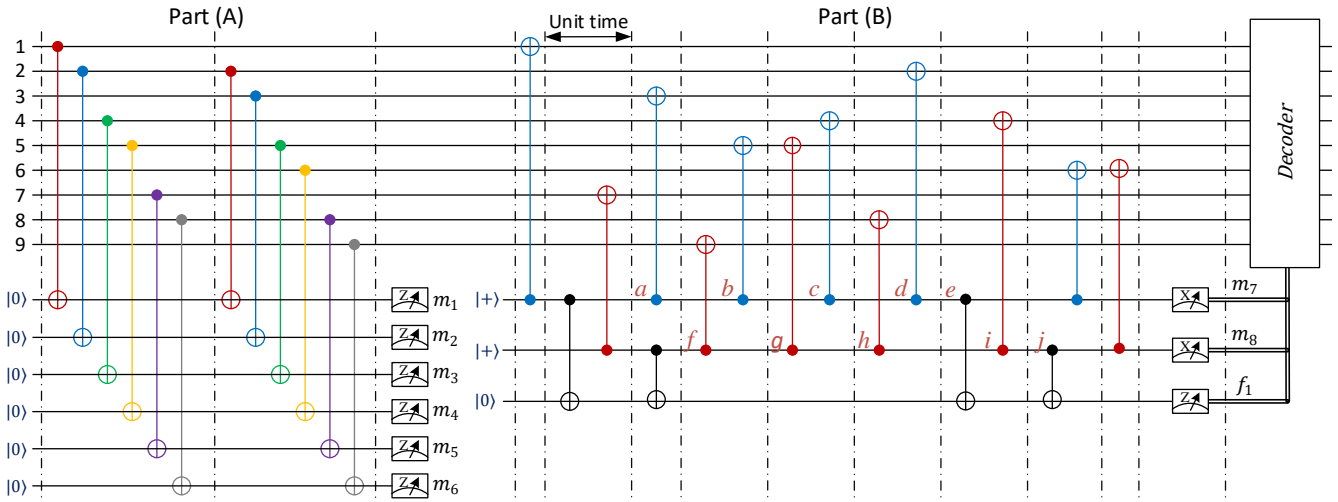


FIG. 4. Parallel flagged syndrome extraction circuit for Shor's  $[[9,1,3]]$  code with one shared flag qubit. Part(A) extracts the syndrome bits for  $Z_1Z_2$  (red),  $Z_2Z_3$  (blue),  $Z_4Z_5$  (green),  $Z_5Z_6$  (yellow),  $Z_7Z_8$  (purple) and  $Z_8Z_9$  (gray). Part (B) extracts the syndrome bits for  $X_1X_2X_3X_4X_5X_6$  (blue) and  $X_4X_5X_6X_7X_8X_9$  (red).

location failure can be detected. Since a bad location failure will trigger the flag qubit in a flagged syndrome extraction circuit, we have the following result.

**Lemma 10** All the  $Z$ -stabilizers of a CSS code of distance two or three can be fault-tolerantly measured in parallel with a shared flag qubit for error detection. Similarly for the  $X$ -stabilizers.

### 1. Shor's $[[9,1,3]]$ code

Shor's  $[[9,1,3]]$  code is constructed by concatenating a three-qubit phase-flip code with a three-qubit bit-flip QECC and can correct an arbitrary  $X$  error and an arbitrary  $Z$  error simultaneously [29]. It is defined by stabilizers

$$\begin{aligned}
 g_1 &= Z_1Z_2, g_2 = Z_2Z_3, g_3 = Z_4Z_5, \\
 g_4 &= Z_5Z_6, g_5 = Z_7Z_8, g_6 = Z_8Z_9, \\
 g_7 &= X_1X_2X_3X_4X_5X_6, \\
 g_8 &= X_4X_5X_6X_7X_8X_9.
 \end{aligned} \tag{1}$$

Since each of  $g_1, g_2, g_3, g_4, g_5$  and  $g_6$  has weight two, its syndrome extraction circuit consists of two CNOTs. One can check that it has no bad location and no flag qubit is required. They can be measured in parallel as shown in Part (A) of Fig. (4).

The two stabilizers  $g_7$  and  $g_8$  can be fault-tolerantly measured using a parallel flagged syndrome extraction circuit by Algorithm 2. There are five location failures in  $C(g_7)$  (or  $C(g_8)$ ) that trigger the flag qubits, which satisfies Proposition 7 with equality. Since there are six  $Z$ -stabilizers, Proposition 9 holds with  $10 < 2^6 = 64$ . Consequently, a parallel syndrome extraction circuit can be easily found as shown in Part (B) of Fig. (4).

By Lemma 11 and Algorithm 3 in the next subsection, the unflagged syndrome extraction circuit consists of solely Part (A) of Fig. 4. The location failures are listed in Table (I), together with their error syndromes from a following separate unflagged syndrome extraction circuit.

Failure	Data error	$m_7m_8f_1$	$m'_{123456}$
$X_a$	$X_{2,3,4,5,6}$	001	100000
$X_b$	$X_{2,4,5,6}$	001	110000
$X_c$	$X_{2,4,6}$	001	111100
$X_d$	$X_{2,6}$	001	110100
$X_e$	$X_6$	001	000100
$X_f$	$X_{4,5,6,8,9}$	001	000010
$X_g$	$X_{4,5,6,8}$	001	000011
$X_h$	$X_{4,6,8}$	001	001111
$X_i$	$X_{4,6}$	001	001100
$X_j$	$X_4$	001	001000

TABLE I. The syndrome table of the syndrome extraction circuit for the  $[[9,1,3]]$  code in Part (B) of Fig. (4) when the flag qubit raises.  $m_7m_8f_1$  denotes the measurement outcomes in Part (B) and  $m'_{123456}$  denotes the measurement outcomes of a following separate unflagged syndrome extraction circuit.

### 2. The $[[15,1,3]]$ Reed-Muller code

The  $[[15,1,3]]$  Reed-Muller code is defined by stabilizers

$$\begin{aligned}
 g_1 &= Z_{1,3,5,7,9,11,13,15}, g_6 = Z_{5,7,13,15}, g_{10} = Z_{9,11,13,15} \\
 g_2 &= Z_{2,3,6,7,10,11,14,15}, g_5 = Z_{3,7,11,15}, g_8 = Z_{10,11,14,15}, \\
 g_3 &= Z_{4,5,6,7,12,13,14,15}, g_7 = Z_{6,7,14,15}, \\
 g_4 &= Z_{8,9,10,11,12,13,14,15}, g_9 = Z_{12,13,14,15}, \\
 g_{11} &= X_{1,3,5,7,9,11,13,15}, g_{12} = X_{2,3,6,7,10,11,14,15}, \\
 g_{13} &= X_{4,5,6,7,12,13,14,15}, g_{14} = X_{8,9,10,11,12,13,14,15}.
 \end{aligned}$$

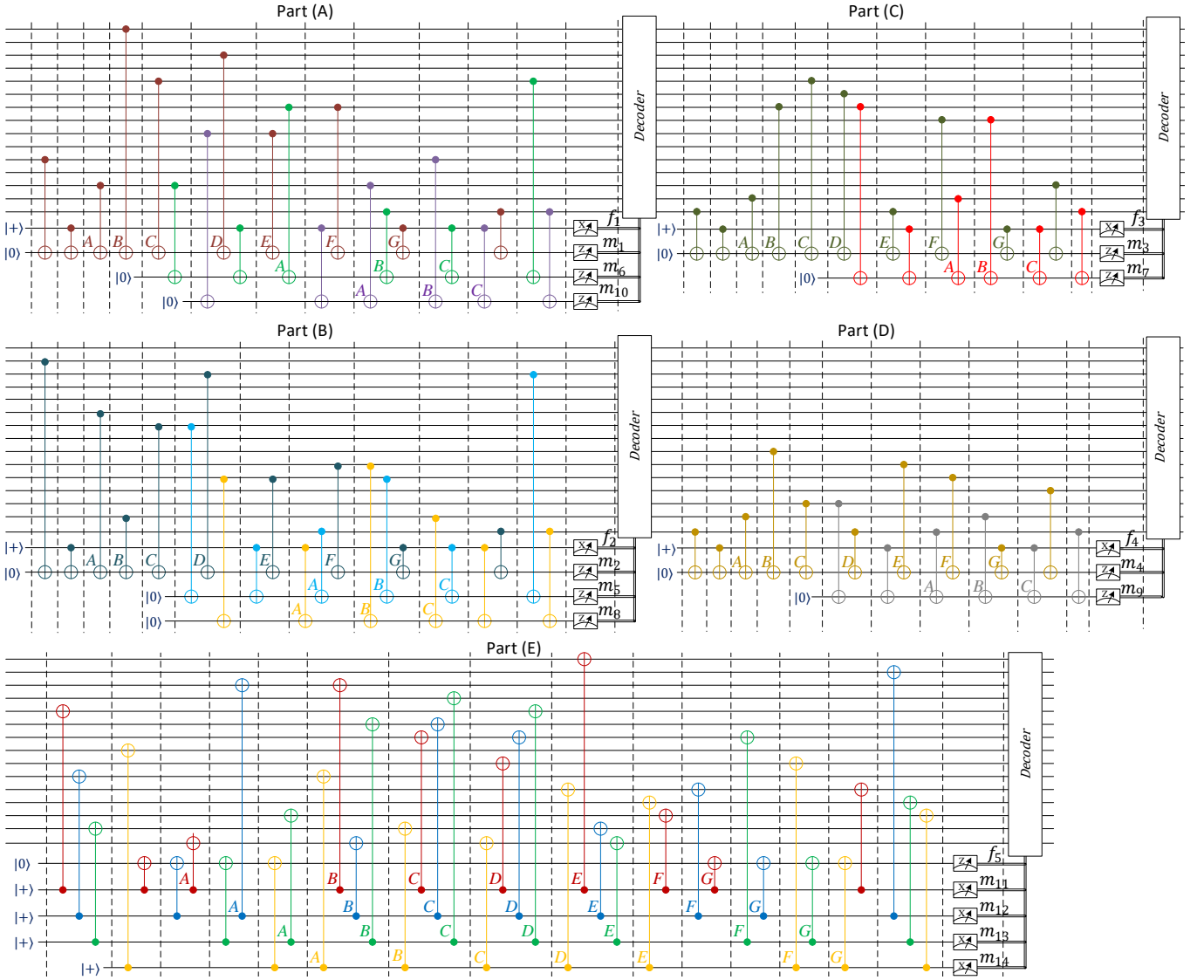


FIG. 5. Circuit of the  $[[15,1,3]]$  code of parallel extraction scheme. Part (A) simultaneously extracts the syndrome for  $g_1, g_6$ , and  $g_{10}$ . Part (B) simultaneously extracts the syndrome for  $g_2, g_5$ , and  $g_8$ . Part (C) simultaneously extracts the syndrome for  $g_3$ , and  $g_7$ . Part (D) simultaneously extracts the syndrome for  $g_4$ , and  $g_9$ . Part (E) simultaneously extracts the syndrome for  $g_{11}, g_{12}, g_{13}$  and  $g_{14}$ . Note that the different colors correspond to different stabilizers.

There are ten  $Z$ -stabilizers  $g_1, \dots, g_{10}$  and four  $X$ -stabilizers  $g_{11}, \dots, g_{14}$  of weight four or eight. By Propositions 7 and 9, we can have at most three  $Z$ -stabilizers measured in parallel with one shared flag qubit, whereas the four  $X$ -stabilizers can be easily measured in parallel with one shared flag qubit. The resulting parallel syndrome extraction circuit is shown in Fig. 5 where Part (A) measures  $g_1, g_6$  and  $g_{10}$ , Part (B) measures  $g_2, g_5$  and  $g_8$ , Part (C) measures  $g_3$  and  $g_7$ , Part (D) measures  $g_4$  and  $g_9$ , and Part (E) measures  $g_{11}, g_{12}, g_{13}$  and  $g_{14}$ . Each stabilizer measurement in each part is differently colored. One can verify that each bad location failure has a unique error syndrome when a flag rises, and the syndrome table is omitted.

## B. Decoding procedures

Finally, we propose a decoding procedure for flagged syndrome extraction of a CSS code. We begin with the following lemma.

**Lemma 11** A location failure in a flagged syndrome extraction circuit of an  $X$ -stabilizer (respectively,  $Z$ -stabilizer) will leave solely  $X$  (respectively,  $Z$ ) errors and possibly a  $Z$  (respectively,  $X$ ) error on the data qubits.

**Proof.** Consider the flagged syndrome extraction circuit in Fig. 3. Consider a location failure at one of the CNOTs that triggers the flag qubit. It may generate a Pauli error on the control (data) qubit and a  $Z$  error on the target (ancillary) qubit, and this  $Z$  error will

---

**Algorithm 3:** Decoding procedure for flagged syndrome extraction of a CSS code.

---

- 1 Suppose that a CSS code of distance three has  $X$ -stabilizers  $g_1^X, \dots, g_x^X$  and  $Z$ -stabilizers  $g_1^Z, \dots, g_z^Z$ ;
- 2  $f_X$  is initialized to  $0^r$ , where  $r$  is the number of flag qubits in  $C(g_1^X), \dots, C(g_x^X)$ ;
- 3 Apply  $C(g_1^X), \dots, C(g_x^X)$  to get the  $Z$  error syndrome bits  $m_X \in \{0, 1\}^x$ ;
- 4 Update  $f_X$  according to the measurement outcomes of the flag qubits in  $C(g_1^X), \dots, C(g_x^X)$ ;
- 5 **if**  $f_X \neq 0^r$  **then**
- 6     Apply a separate unflagged syndrome extraction circuit for the  $Z$ -stabilizers to get syndrome bits  $m'_Z \in \{0, 1\}^z$ ;
- 7     Perform error correction according to  $\text{LOOKUP}(f)$  and  $m'_Z$ ;
- 8 **else if**  $f_X = 0^r$  **and**  $m_X \neq 0^x$  **then**
- 9     Apply a complete unflagged syndrome extraction circuit to get syndrome bits  $m' \in \{0, 1\}^{x+z}$ ;
- 10    Perform error correction according to  $\text{LOOKUP}(0)$  and  $m'$ ;
- 11 **else if**  $f_X = 0^r$  **and**  $m_X = 0^x$  **then**
- 12     $f_Z$  is initialized to  $0^s$ , where  $s$  is the number of flag qubits in  $C(g_1^Z), \dots, C(g_z^Z)$ ;
- 13    Apply  $C(g_1^Z), \dots, C(g_z^Z)$  to get the  $X$  error syndrome  $m_Z \in \{0, 1\}^z$ ;
- 14    **if**  $f_Z \neq 0^s$  **then**
- 15     Apply a separate unflagged syndrome extraction circuit for the  $X$ -stabilizers to get syndrome bits  $m'_X \in \{0, 1\}^x$ ;
- 16     Perform error correction according to  $\text{LOOKUP}(f)$  and  $m'_X$ ;
- 17     **else if**  $m_Z \neq 0^z$  **then**
- 18     Apply a separate unflagged syndrome extraction circuit for the  $Z$ -stabilizers to get syndrome bits  $m'_Z \in \{0, 1\}^z$ ;
- 19     Perform error correction according to  $\text{LOOKUP}(0)$  and  $m'_Z$ ;
- 20    **end**
- 21 **end**

---

propagate to multiple data qubits. The condition is similar for the syndrome extraction of a  $Z$ -stabilizer.

Note that in Fig. 3, a bad location failure will trigger the flag qubit, and the high-weight  $Z$  error can be detected by measuring the  $X$ -stabilizers. Meanwhile, a possible residual  $X$  error can be detected and corrected by measuring the  $Z$ -stabilizers.

We remark that this residual  $X$  error can be left uncorrected to the next error correction cycle, whereas the syndrome extraction procedure remains to be fault-tolerant. This suggests a decoding procedure for CSS codes as shown in Algorithm 3, where separate unflagged syndrome extractions for  $X$  and  $Z$  stabilizers are applied, respectively. Since we do not perform a complete syndrome extraction, the overhead for FTQC can be greatly reduced.

---

**Algorithm 4:** (Symmetric) Decoding procedure for flagged syndrome extraction of a CSS code.

---

- 1 Suppose a that CSS code of distance three has  $X$ -stabilizers  $g_1^X, \dots, g_x^X$  and  $Z$ -stabilizers  $g_1^Z, \dots, g_z^Z$ ;
- 2  $f_X$  is initialized to  $0^r$ , where  $r$  is the number of flag qubits in  $C(g_1^X), \dots, C(g_x^X)$ ;
- 3 Apply  $C(g_1^X), \dots, C(g_x^X)$  to get the  $Z$  error syndrome bits  $m_X \in \{0, 1\}^x$ ;
- 4 Update  $f_X$  according to the measurement outcomes of the flag qubits in  $C(g_1^X), \dots, C(g_x^X)$ ;
- 5 **if**  $f_X \neq 0^r$  **then**
- 6     Apply a separate unflagged syndrome extraction circuit for the  $Z$ -stabilizers to get syndrome bits  $m'_Z \in \{0, 1\}^z$ ;
- 7     Perform error correction according to  $\text{LOOKUP}(f)$  and  $m'_Z$ ;
- 8 **else if**  $f_X \neq 0^r$  **and**  $m_X \neq 0^x$  **then**
- 9     Apply a separate unflagged syndrome extraction circuit to get syndrome bits  $m'_X \in \{0, 1\}^x$ ;
- 10    Perform error correction according to  $\text{LOOKUP}(0)$  and  $m'_X$ ;
- 11 **end**
- 12  $f_Z$  is initialized to  $0^s$ , where  $s$  is the number of flag qubits in  $C(g_1^Z), \dots, C(g_z^Z)$ ;
- 13 Apply  $C(g_1^Z), \dots, C(g_z^Z)$  to get the  $X$  error syndrome  $m_Z \in \{0, 1\}^z$ ;
- 14 **if**  $f_Z \neq 0^s$  **then**
- 15     Apply a separate unflagged syndrome extraction circuit for the  $X$ -stabilizers to get syndrome bits  $m'_X \in \{0, 1\}^x$ ;
- 16     Perform error correction according to  $\text{LOOKUP}(f)$  and  $m'_X$ ;
- 17 **else if**  $f_X \neq 0^r$  **and**  $m_Z \neq 0^z$  **then**
- 18     Apply a separate unflagged syndrome extraction circuit for the  $Z$ -stabilizers to get syndrome bits  $m'_Z \in \{0, 1\}^z$ ;
- 19     Perform error correction according to  $\text{LOOKUP}(0)$  and  $m'_Z$ ;
- 20 **end**

---

We remark that  $X$  and  $Z$  errors are differently treated in Algorithm 3. In a sequence of error correction cycles, we may alternate the order of  $X$  and  $Z$  treatments in each cycle.

As a comparison, we also provide Algorithm 4, where  $X$  and  $Z$  errors are symmetrically treated. These two decoding algorithms will be compared in the next section, where we show by simulations that Algorithm 3 performs slightly better.

#### IV. SIMULATION RESULTS

In this section, we simulate the memory and computation thresholds of the error detection scheme based on the  $[[4,2,2]]$  code with standard and parallel flagged syndrome extraction, respectively, the scheme based on the  $[[7,1,3]]$  Steane code with parallel syndrome extraction,



and the scheme based on Shor’s  $[[9,1,3]]$  code with parallel syndrome extraction.

We consider depolarizing errors. We assume that all the gates have the same error rate and the ratio of memory error rate (idle qubits) to the gate error rate is  $\gamma$ . Simulations will be conducted at  $\gamma = 0$  and  $\gamma = 1$ .

The number of locations in an ex-Rec CNOT gate of each scheme is provided in Table II. Note that the  $[[4,2,2]]$ ,  $[[7,1,3]]$ , and  $[[9,1,3]]$  flag schemes follow the standard flagged syndrome extraction in Algorithm 1; the  $[[4,2,2]]$ ,  $[[7,1,3]]$  parallel schemes are given in Ref. [27]; the  $[[9,1,3]]$  parallel scheme is proposed in Section III A 1 with the decoding procedure in Algorithm 3. Our code can be found in Ref. [37].

	$[[4,2,2]]$ Flag	$[[4,2,2]]$ Parallel	$[[7,1,3]]$ Flag <sup>a</sup>	$[[7,1,3]]$ Parallel <sup>a</sup>	$[[9,1,3]]$ Flag <sup>a</sup>	$[[9,1,3]]$ Parallel <sup>a</sup>
$P_s$ <sup>b</sup>	16	8	264	72	176	100
$M_X$	8	4	132	36	24	24
$M_Z$	8	4	132	36	152	76
CNOT	52	36	1015	343	457	313
Idle qubit	192	64	6360	824	1688	1284
SWAP	0	8	0	0	0	0
Total	276	124	7903	1311	2497	1797

<sup>a</sup> These numbers are overestimated since the locations in all the unflagged syndrome extraction circuits are counted.

<sup>b</sup>  $P_s$  denotes ancilla state preparation.

TABLE II. The number of locations in an ex-Rec CNOT gate for various schemes.

### A. Comparisons of procedures for unflagged syndrome extraction

We proposed Algorithms 3 and 4 for CSS codes so that a complete unflagged syndrome extraction is not required for CSS codes when some flag qubits rise. In this subsection, we demonstrate this on the parallel flagged syndrome extraction for the error correction scheme based on the  $[[9,1,3]]$  code proposed in Section III A 1.

The memory and computation pseudo-thresholds using the decoding procedure in Algorithm 4 with complete unflagged syndrome extraction or Algorithms 3 and 4 with separate unflagged syndrome extraction are summarized in Table III. The results show that using a separate and nonsymmetric unflagged syndrome extraction by Algorithm 3 is better in all respects. Consequently, we will adopt this strategy in the following simulations.

### B. Error detection

Simulations of the  $[[4,2,2]]$ ,  $[[7,1,3]]$ , and  $[[9,1,3]]$  codes with error detection are given in Fig. 6. The  $[[4,2,2]]$ ,  $[[7,1,3]]$ , and  $[[9,1,3]]$  flag schemes are with standard flagged syndrome extraction; the  $[[4,2,2]]$ ,  $[[7,1,3]]$  parallel schemes are given in [27] and can be

$[[9,1,3]]$ Parallel Scheme	$\gamma = 0$	$\gamma = 1$
Decoding Procedure	Memory pseudo-threshold	
Alg. 4 with comp.	$8.01 \times 10^{-3}$	$8.3 \times 10^{-4}$
Alg. 4	$8.06 \times 10^{-3}$	$8.52 \times 10^{-4}$
Alg. 3	$9.82 \times 10^{-3}$	$8.84 \times 10^{-4}$
Decoding Procedure	Computation pseudo-threshold	
Alg. 4 with comp.	$3.94 \times 10^{-4}$	$3.35 \times 10^{-5}$
Alg. 4	$4.19 \times 10^{-4}$	$4.97 \times 10^{-5}$
Alg. 3	$7.81 \times 10^{-4}$	$8.11 \times 10^{-5}$

TABLE III. Comparisons of the three procedures for unflagged syndrome extraction. Note that Alg. 3 and Alg. 4 are the  $X$  and  $Z$  separate unflagged syndrome extraction, while Alg. 4 with comp. uses a complete unflagged syndrome extraction instead.

found in Appendix A; the  $[[9,1,3]]$  Parallel is the scheme proposed in Section III A 1.

Figures 6 (a) and (b) provide the memory pseudo-thresholds at  $\gamma = 0$  and  $\gamma = 1$ , respectively, while Figures 6 (c) and (d) provide the computation pseudo-thresholds at  $\gamma = 0$  and  $\gamma = 1$ , respectively.

In general, the flag and parallel schemes have comparable pseudo-thresholds at  $\gamma = 0$ . At  $\gamma = 1$ , the advantages of parallel scheme is more obvious as expected since it has fewer qubits and gates involved.

At  $\gamma = 0$ , both the  $[[7,1,3]]$  and  $[[9,1,3]]$  codes have computation pseudo-thresholds around 5%, while their memory pseudo-thresholds are above 10%. At  $\gamma = 1$ , the  $[[7,1,3]]$  parallel is slightly better than the  $[[9,1,3]]$  parallel scheme for error detection.

### C. Error correction

Simulations of the  $[[7,1,3]]$  and  $[[9,1,3]]$  codes with error correction are given in Fig. 7.

We first consider the memory pseudo-threshold of the  $[[7,1,3]]$  and  $[[9,1,3]]$  schemes using Algorithm 3 for error correction, which are shown in Fig. 7 (a) and (b), respectively. The memory and computation pseudo-thresholds for these schemes using Algorithm 3 are summarized in Table IV.

As a comparison, we include the pseudo-threshold of the  $[[7,1,3]]$  flag scheme using a two-round decoder in [23], which has a better threshold than the  $[[7,1,3]]$  flag scheme using the standard decoder.

We also compare our  $[[9,1,3]]$  parallel scheme with the *Bacon-Shor-13* scheme in Ref. [19]. For a fair comparison, we reproduce their results and simulate the memory pseudo-threshold for the Bacon-Shor-13 scheme at  $\gamma = 0$  and  $\gamma = 1$  based on the circuit for Bacon-Shor-13 in Fig. 8 and the results are also shown in Table IV and Fig. 7 (a).

It is obvious from the simulations that the parallel schemes are much better than their flag counterparts since the parallel schemes have fewer qubits and gates as can be observed from Table II.

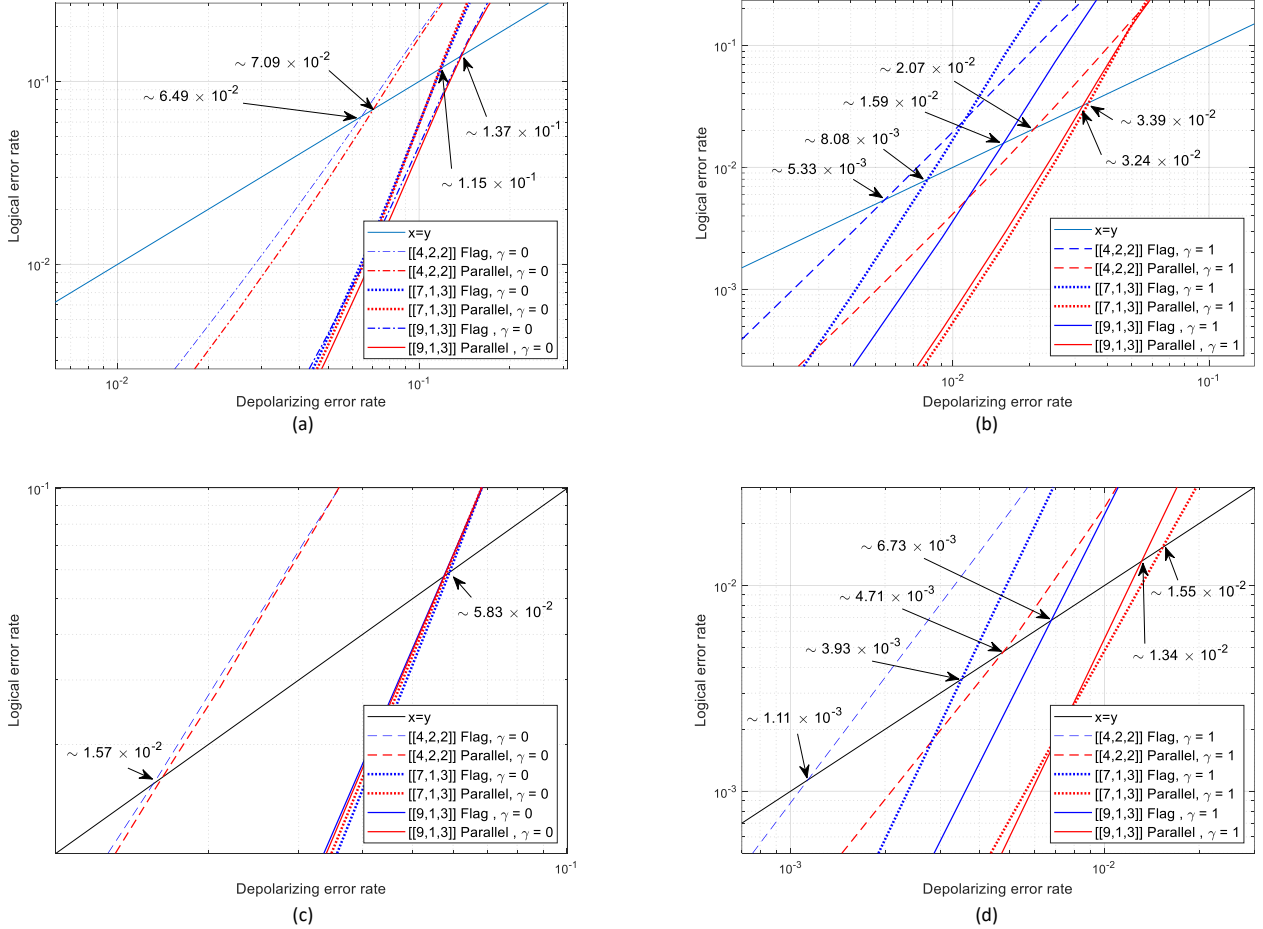


FIG. 6. Error correction: simulations of the memory and computation pseudo-thresholds for various schemes at  $\gamma = 0$  and  $\gamma = 1$ , using Algorithm 3. (a) Memory pseudo-thresholds at  $\gamma = 0$ . (b) Memory pseudo-thresholds at  $\gamma = 1$ . (c) Computation pseudo-thresholds at  $\gamma = 0$ . (d) Computation pseudo-thresholds at  $\gamma = 1$ .

Remarkably, our  $[[9,1,3]]$  parallel scheme has the highest memory pseudo-thresholds of  $9.82 \times 10^{-3}$  and  $8.84 \times 10^{-4}$  at  $\gamma = 0$  and  $\gamma = 1$ , respectively, among these schemes.

The simulation results for the computation pseudo-thresholds using Algorithm 3 have similar behaviors as shown in Fig. 7 (b). Our  $[[9,1,3]]$  parallel scheme also outperforms the  $[[7,1,3]]$  parallel scheme in the computation pseudo-threshold.

## V. CONCLUSION

We proposed a general parallel flagged syndrome extraction scheme for a CSS code of distance three with one shared flag qubit (Algorithm 2), together with a decoding procedure for separate unflagged syndrome extraction (Algorithm 3). Examples of the  $[[9,1,3]]$  Shor and  $[[15,1,3]]$  Reed-Muller codes were provided.

Simulations on the  $[[9,1,3]]$  code demonstrated that our  $[[9,1,3]]$  parallel scheme has several benefits over

	$\gamma = 0$	$\gamma = 1$
Scheme	Memory pseudo-threshold	
$[[7, 1, 3]]$ flag	$8.31 \times 10^{-4}$	$2.53 \times 10^{-5}$
$[[7, 1, 3]]$ flag	—	$3.39 \times 10^{-5}$ [23] <sup>a</sup>
$[[7, 1, 3]]$ parallel [27]	$1.29 \times 10^{-3}$	$1.75 \times 10^{-4}$
$[[9, 1, 3]]$ flag	$7.41 \times 10^{-3}$	$3.18 \times 10^{-4}$
$[[9, 1, 3]]$ parallel	$9.82 \times 10^{-3}$	$8.84 \times 10^{-4}$
Bacon-Shor-13 [19]	$8.57 \times 10^{-3}$ [19]	$6.21 \times 10^{-4}$ [19]
Scheme	Computation pseudo-threshold	
$[[7, 1, 3]]$ flag	$2.07 \times 10^{-4}$	$7.38 \times 10^{-6}$
$[[7, 1, 3]]$ parallel [27]	$1.73 \times 10^{-4}$	$3.02 \times 10^{-5}$
$[[9, 1, 3]]$ flag	$4.31 \times 10^{-4}$	$2.09 \times 10^{-5}$
$[[9, 1, 3]]$ parallel	$7.81 \times 10^{-4}$	$8.11 \times 10^{-5}$

<sup>a</sup> A two-round decoder is used.

TABLE IV. Memory and computation pseudo-thresholds for various schemes of the  $[[7, 1, 3]]$  and  $[[9, 1, 3]]$  codes.

the  $[[7,1,3]]$  code. Also it has a high memory pseudo-threshold around  $8.84 \times 10^{-4}$ , assuming all the gates

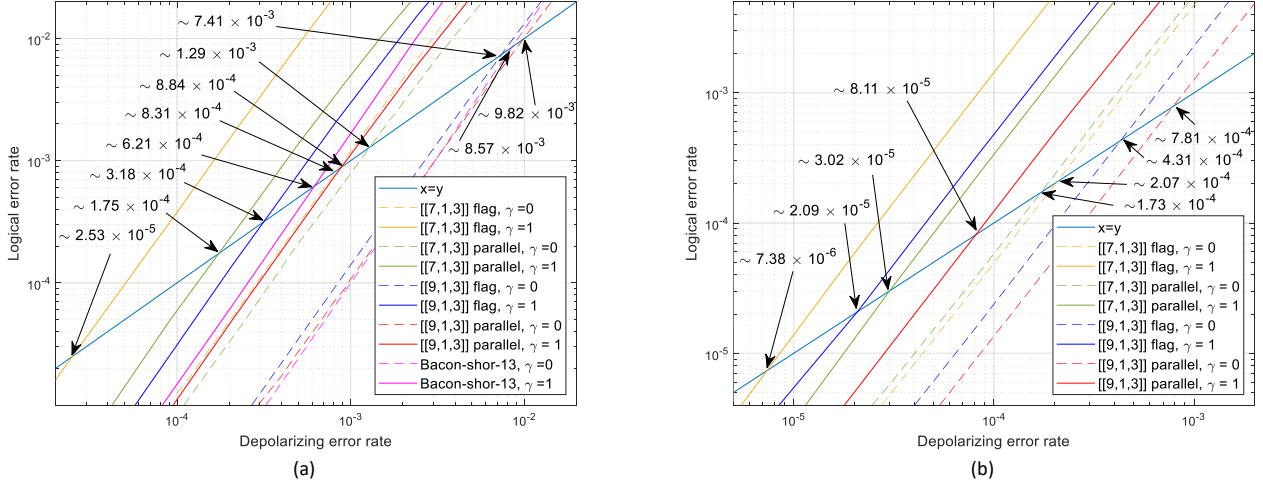


FIG. 7. Error correction: simulations of the memory and computation pseudo-thresholds for various schemes at  $\gamma = 0$  and  $\gamma = 1$ , using Algorithm 3. (a) Memory pseudo-thresholds. (b) Computation pseudo-thresholds.

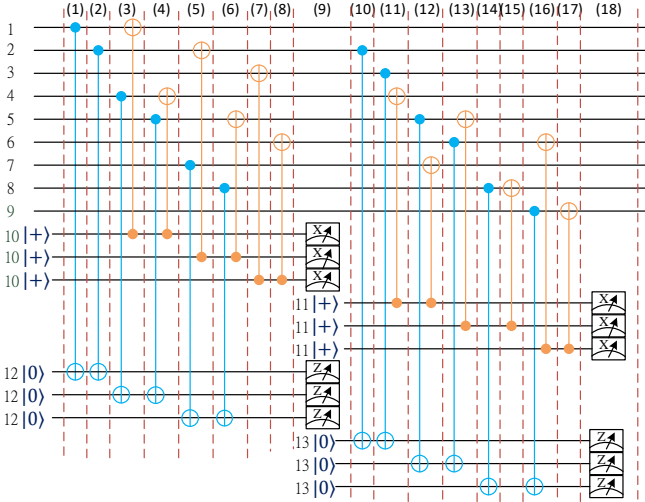


FIG. 8. The circuit for the Bacon-Shor-13 scheme.

and memory have the same error rate. The  $[[9,1,3]]$  parallel scheme uses six ancillas for the  $Z$ -stabilizer measurements, where three ancillas can be reset for the  $X$ -stabilizer measurements in the second part. It is also better than Bacon-Shor-13 at the cost of two additional qubits for parallelism. Since Bacon-Shor-13 uses only four ancilla qubits for syndrome extraction, it has long circuit depth and many idle qubit locations.

Our procedure works for CSS codes. However, there are examples of non-CSS codes with shared flag qubits in Refs. [21, 27]. A procedure for a general stabilizer code maybe be possible but it is beyond our scope.

In Ref. [38], Lao and Almudever proposed a two-dimensional layout for the  $[[7,1,3]]$  Steane code with a shared flag qubit [21]. In particular, they consider a variant of the standard flagged syndrome extraction to reduce the circuit depth. Consequently, the CNOT gates

for a stabilizer measurement may be equally connect to an ancilla qubit and the flag qubit. The circuit depth can be decreased in this way. However, it may not be easy to have parallel syndrome extraction for multiple stabilizers with one shared flag qubit since it will be difficult to find an arrangement of the CNOT gates such that each bad location failure will have a unique error syndrome.

We consider only quantum codes of distance two and three in this paper. It is possible to extend our framework for CSS codes of higher distances, where more shared flag qubits are required. However, it is difficult to arrange the CNOTs so that each bad location failure will have a unique error syndrome by a complete unflagged syndrome extraction.

## ACKNOWLEDGMENTS

CYL was supported by the National Science and Technology Council (NSTC) in Taiwan, under Grants No. NSTC110-2628-E-A49-007, No. NSTC111-2119-M-A49-004, and No. NSTC111-2119-M-001-002.

## Appendix A: Parallel flagged syndrome extraction of the $[[4, 2, 2]]$ and $[[7, 1, 3]]$ codes

We explain Reichardt's parallel syndrome extraction with flag qubits [27] in the following. Figure 9 shows a parallel syndrome extraction circuit for the  $[[4, 2, 2]]$  code, whose circuit depth is lower than the cascade form in Fig. 1. Only two ancilla qubits are used to extract two syndrome bits, and each of them serves as a flag qubit for the other. Note that two SWAP gates are introduced, instead of CNOT gates.

Each single location failure in the parallel circuit Fig. 9 and its resulting data error are provided in Table V,

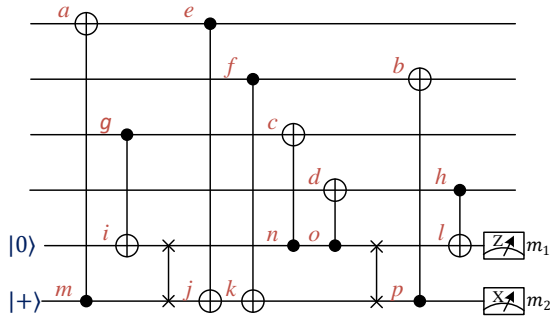


FIG. 9. Parallel syndrome extraction<sup>a</sup> of  $X_1X_2X_3X_4$  and  $Z_1Z_2Z_3Z_4$  for the  $[[4,2,2]]$  code.

<sup>a</sup> This circuit is a modification of the circuit in [27] so that the code space is preserved.

Failure	Data error	$m_{1,2}$	Failure	Data error	$m_{1,2}$
$X_a$	$X_1$	10	$Z_a$	$Z_1$	01
$X_b$	$X_2$	00	$Z_b$	$Z_2$	01
$X_c$	$X_3$	00	$Z_c$	$Z_3$	01
$X_d$	$X_4$	10	$Z_d$	$Z_4$	01
$X_e$	$X_1$	10	$Z_e$	$Z_1$	00
$X_f$	$X_2$	10	$Z_f$	$Z_2$	01
$X_g$	$X_3$	10	$Z_g$	$Z_3$	01
$X_h$	$X_4$	10	$Z_h$	$Z_4$	00
$X_i$	None	10	$Z_i$	$Z_{1,2,3,4}$	00
$X_j$	None	10	$Z_j$	$Z_{1,2,4}$	01
$X_k$	None	10	$Z_k$	$Z_{2,4}$	01
$X_l$	None	10	$Z_l$	$Z_4$	00
$X_m$	$X_{1,2,3,4}$	00	$Z_m$	None	01
$X_n$	$X_{2,3,4}$	10	$Z_n$	None	01
$X_o$	$X_{2,4}$	10	$Z_o$	None	01
$X_p$	$X_2$	00	$Z_p$	None	01

TABLE V. Equivalent errors on the data qubits for various single location failures and their syndromes in the parallel syndrome extraction circuit of  $X_1X_2X_3X_4$  and  $Z_1Z_2Z_3Z_4$  in Fig. 9 for the  $[[4,2,2]]$  code.

where  $X_a$  or  $Z_a$  denotes a corresponding Pauli error at location  $a$ . A few notes on the table are as follows. The ancilla failures, such as  $X_i$  and  $Z_m$  do not introduce any data qubit errors; however, they cannot be identified from the syndromes and the uncorrupted codewords have to be discarded. On the other hand,  $X_m$  and  $Z_i$  induce certain data errors that are stabilizer generators and hence the data qubits are not affected. Certain failures, such as  $X_p$  and  $Z_l$  induce weight-1 errors with zero

syndrome, but these errors will be detected and corrected in the next round of error detection.

Next we explain parallel syndrome extraction with shared flag qubits for the  $[[7,1,3]]$  Steane code [35], which is defined by the following stabilizer generators

$$\begin{aligned} X_1X_3X_5X_7, & Z_2Z_3Z_6Z_7, & Z_4Z_5Z_6Z_7, \\ Z_1Z_3Z_5Z_7, & X_2X_3X_6X_7, & X_4X_5X_6X_7. \end{aligned} \quad (\text{A1})$$

Reichardt demonstrated that two or three stabilizer generators in Eq. (A1) can be simultaneously measured in

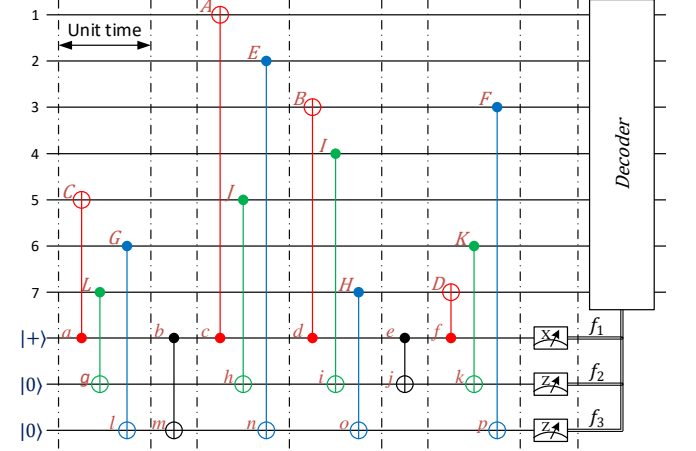


FIG. 10. Parallel syndrome extraction circuits for the  $[[7,1,3]]$  code. (A):  $X_1X_3X_5X_7$  (red),  $Z_2Z_3Z_6Z_7$  (blue), and  $Z_4Z_5Z_6Z_7$  (green). (B):  $Z_1Z_3Z_5Z_7$ ,  $X_2X_3X_6X_7$ , and  $X_4X_5X_6X_7$ .

a fault-tolerant way [27]. Figure (10) illustrates the case of measuring three stabilizers  $X_1X_3X_5X_7$ ,  $Z_2Z_3Z_6Z_7$ , and  $Z_4Z_5Z_6Z_7$  in parallel and only three ancillas are required [27]. The two additional CNOTs connecting the ancillas are elegantly placed so that each of the ancillas can serve as a flag qubit for the others.

Unlike our protocol, a complete unflagged syndrome extraction circuit is applied here if anyone of the binary measurement outcomes  $f_1, f_2, f_3$  is 1. To reduce the circuit depth, one can apply an unflagged version of Fig. (10) to extract the three syndrome bits and similarly for the other three.

The idea of shared flag qubits also works for the  $[[5,1,3]]$  code and the  $[[15,7,3]]$  CSS code so that two stabilizers can be simultaneously measured but an extra flag qubit is necessary [27].

[1] M. Takita, A. W. Cross, A. D. Córcoles, J. M. Chow, and J. M. Gambetta, Experimental demonstration of fault-tolerant state preparation with superconducting qubits, *Phys. Rev. Lett.* **119**, 180501 (2017).  
[2] C. Vuillot, Is error detection helpful on IBM 5Q chips?, *Quantum information & computation* **18**, 0949 (2018).  
[3] L. Postler, S. Heußen, I. Pogorelov, M. Rispler, T. Feld-

ker, M. Meth, C. D. Marciniak, R. Stricker, M. Ringbauer, R. Blatt, P. Schindler, M. Müller, and T. Monz, Demonstration of fault-tolerant universal quantum gate operations (2022).  
[4] L. Egan, D. M. Debroy, C. Noel, A. Risinger, D. Zhu, D. Biswas, M. Newman, M. Li, K. R. Brown, M. Cetina, and C. Monroe, Fault-tolerant control of an error-

- corrected qubit, *Nature* **598**, 281 (2021).
- [5] D. Aharonov and M. Ben-Or, Fault-tolerant quantum computation with constant error, in *Proceedings of the twenty-ninth annual ACM symposium on Theory of computing*, STOC '97 (ACM, New York, NY, USA, 1997) pp. 176–188.
- [6] P. W. Shor, Fault-tolerant quantum computation, in *Proceedings of the 37th Annual Symposium on the Theory of Computer Science* (IEEE Press, Los Alamitos, 1996) pp. 56–65.
- [7] D. P. DiVincenzo and P. W. Shor, Fault-tolerant error correction with efficient quantum codes, *Phys. Rev. Lett.* **77**, 3260 (1996).
- [8] E. Knill, R. Laflamme, and W. Zurek, Threshold accuracy for quantum computation 10.48550/ARXIV.QUANT-PH/9610011 (1996).
- [9] D. Gottesman, *Stabilizer codes and quantum error correction*, Ph.D. thesis, California Institute of Technology, Pasadena, CA (1997).
- [10] J. Preskill, Reliable quantum computers (Proc. R. Soc. Lond. A, 1998) pp. 385–410.
- [11] A. M. Steane, Active stabilization quantum computation, and quantum state synthesis, *Phys. Rev. Lett.* **78**, 2252 (1997).
- [12] A. M. Steane, Efficient fault-tolerant quantum computing, *Nature* **399**, 124 (1999).
- [13] E. Knill, Quantum computing with realistically noisy devices, *Nature* **434**, 39 (2005).
- [14] A. Ashikhmin, C.-Y. Lai, and T. A. Brun, Quantum data-syndrome codes, *IEEE J. Sel. Area. Comm.* **38**, 449 (2020).
- [15] K.-Y. Kuo, I.-C. Chern, , and C.-Y. Lai, Decoding of quantum data-syndrome codes via belief propagation, in *2021 IEEE International Symposium on Information Theory (ISIT)* (2021) pp. 1552–1557.
- [16] Y.-C. Zheng, C.-Y. Lai, T. A. Brun, and L.-C. Kwek, Constant depth fault-tolerant Clifford circuits for multi-qubit large block codes, *Quant. Sci. Tech.* **5**, 045007 (2020).
- [17] S. Huang and K. R. Brown, Between Shor and Steane: A unifying construction for measuring error syndromes, *Phys. Rev. Lett.* **127**, 090505 (2021).
- [18] A. G. Fowler, M. Mariantoni, J. M. Martinis, and A. N. Cleland, Surface codes: Towards practical large-scale quantum computation, *Phys. Rev. A* **86**, 032324 (2012).
- [19] M. Li, D. Miller, and K. R. Brown, Direct measurement of Bacon-Shor code stabilizers, *Phys. Rev. A* **98**, 050301(R) (2018).
- [20] T. J. Yoder and I. H. Kim, The surface code with a twist, *Quantum* **1**, 2 (2017).
- [21] R. Chao and B. W. Reichardt, Quantum error correction with only two extra qubits, *Phys. Rev. Lett.* **121**, 050502 (2018).
- [22] R. Chao and B. W. Reichardt, Fault-tolerant quantum computation with few qubits, *npj Quantum Inf.* **4**, 42 (2018).
- [23] C. Chamberland and M. E. Beverland, Flag fault-tolerant error correction with arbitrary distance codes, *Quantum* **2**, 53 (2018).
- [24] C. Chamberland and A. W. Cross, Fault-tolerant magic state preparation with flag qubits, *Quantum* **3**, 143 (2019).
- [25] T. Tansuwannont, C. Chamberland, and D. Leung, Flag fault-tolerant error correction, measurement, and quantum computation for cyclic Calderbank-Shor-Steane codes, *Phys. Rev. A* **101**, 012342 (2020).
- [26] R. Chao and B. W. Reichardt, Flag fault-tolerant error correction for any stabilizer code, *PRX Quantum* **1**, 010302 (2020).
- [27] B. W. Reichardt, Fault-tolerant quantum error correction for Steane’s seven-qubit color code with few or no extra qubits, *Quantum Sci. Tech.* **6**, 015007 (2021).
- [28] A. M. Steane, Multiple particle interference and quantum error correction, *Proc. R. Soc. London A* **452**, 2551 (1996).
- [29] P. W. Shor, Scheme for reducing decoherence in quantum computer memory, *Phys. Rev. A* **52**, R2493 (1995).
- [30] K. M. Svore, D. P. Divincenzo, and B. M. Terhal, Noise threshold for a fault-tolerant two-dimensional lattice architecture, *Quantum Information & Computation* **7**, 297 (2007).
- [31] F. M. Spedalieri and V. P. Roychowdhury, Latency in local, two-dimensional, fault-tolerant quantum computing, *Quantum Information & Computation* **9**, 666 (2009).
- [32] C.-Y. Lai, G. Paz, M. Suchara, and T. Brun, Performance and error analysis of Knill’s postselection scheme in a two-dimensional architecture, *Quantum Information & Computation* **14**, 807 (2014).
- [33] F. J. MacWilliams and N. J. A. Sloane, *The Theory of Error-Correcting Codes* (North-Holland, Amsterdam, The Netherlands, 1977).
- [34] A. R. Calderbank and P. W. Shor, Good quantum error-correcting codes exist, *Phys. Rev. A* **54**, 1098 (1996).
- [35] A. M. Steane, Error correcting codes in quantum theory, *Phys. Rev. Lett.* **77**, 793 (1996).
- [36] P. Aliferis, D. Gottesman, and J. Preskill, Quantum accuracy threshold for concatenated distance-3 codes, *Quantum Information & Computation* **6**, 97 (2006).
- [37] Pei-hao liou and ching-yi lai, [https://github.com/slorqwq/parallel\\_sf](https://github.com/slorqwq/parallel_sf) (2023).
- [38] L. Lao and C. G. Almudever, Fault-tolerant quantum error correction on near-term quantum processors using flag and bridge qubits, *Phys. Rev. A* **101**, 032333 (2020).